

Article

Minimizing the Energy Cost of Offshore Wind Farms by Simultaneously Optimizing Wind Turbines and Their Layout

Longfu Luo ¹, Xiaofeng Zhang ¹, Dongran Song ^{2,*} , Weiyi Tang ^{2,*}, Li Li ² and Xiaoyu Tian ²

¹ College of Electrical and Information Engineering, Hunan University, Changsha 410082, China; llf@hnu.edu.cn (L.L.); zxf0303@126.com (X.Z.)

² School of Automation, Central South University, Changsha 410083, China; lili112209@163.com (L.L.); txy15388967580@163.com (X.T.)

* Correspondence: humble_szy@163.com (D.S.); 154601016@csu.edu.cn (W.T.); Tel.: +86-181-636-56151 (D.S.); +86-138-6122-2783 (W.T.)

Received: 23 January 2019; Accepted: 22 February 2019; Published: 26 February 2019



Abstract: The construction and gradual installation of turbines on wind farms has been hindered by the high cost of the energy production. An effective way to minimize energy costs is via the optimal design of wind turbines and their layout, but relevant and synthetic studies are lacking. This paper proposes a method to minimize the energy cost of offshore wind farms by simultaneously optimizing the rated wind speed, the rotor radius of wind turbines and their layout. Firstly, a new, mixed mathematical formulation of the energy cost is presented, considering the Weibull distribution for wind, the characterizing parameters of wind turbines and the distance between two turbines. Secondly, to obtain the minimum energy cost, a composite optimization algorithm was developed, which consists of an iterative method and an improved particle swarm optimization algorithm. The former was used to search the minimal energy costs that relate to the design parameters of a single wind turbine, while the latter was adopted for optimizing the layout of the wind turbines iteratively. Finally, the proposed method was applied to three case studies with variable wind speed and constant wind direction. Results of the case studies show that the reduced energy cost after optimization has a range of 0–0.001 \$/kWh, which confirms the effectiveness of the proposed approach. Meanwhile, the layout of the wind turbines after optimization tends to locate the two wind turbines with the biggest spacing in the wind direction, which justifies the utilization of layout optimization. Furthermore, exploring the optimally designed parameters of wind turbines revealed that the wind farms with a high mean wind speed can have a wider range of turbine capacity than those with a low wind speed, which offers more freedom for the designers when constructing offshore wind farms at wind sites with rich wind resources.

Keywords: offshore wind farm; cost of energy; layout; optimal design; particle swarm optimization

1. Introduction

An offshore wind farm shows more benefit in terms of higher wind speed, less turbulence, unrestricted area and less impact on residents compared with an onshore wind farm [1]. However, the construction of offshore wind farms brings about expensive ocean treatment, plus installation, operation and maintenance costs, which have greatly slowed down the development of wind energy and hindered the construction of offshore wind farms. In order to obtain a cost-effective wind farm, the cost of energy (COE) at offshore wind farms should be optimized. COE is widely used by project developers to evaluate the economic benefit of a project in short, medium and long terms.

As the COE of the whole offshore wind farm is relevant to the total annual cost and the annual energy production (AEP), the COE is optimized by considering two aspects: reducing the production cost and increasing the AEP. Considering the design of the offshore wind farm, the approaches to optimize the COE can be categorized into main two types: wind farm layout optimization (WFLO) and wind turbine design optimization (WTDO). The WFLO aims to study the optimal layout of wind turbines on a certain wind farm, so that the maximum AEP and the minimum cost can be realized. Much existing research revealed that the WFLO has a significant impact on the performance of the offshore wind farm and the total produced energy when using a specific kind of wind turbine. In these studies, WFLO is achieved by considering two main factors: the wake effect and the optimization algorithm. The wake effect has a great influence on the AEP. Wakes from upstream turbines can severely affect the performance of downwind turbines, and the wake losses typically reduce the power generated by 10–20% compared with the undisturbed turbines [2]. In order to describe the complex, non-linear phenomena, many wake loss models have been developed describing the real flow field with relative accuracy. So far, the existing wake loss models can be categorized as Jensen models [3], Larsen models [4], Frandsen models [5], Gaussian models [6] and corresponding extended wake loss models. Among these wake loss models, the Jensen model has been widely applied to describe the turbine wake, for it is a simple model and needs less computational resources. On the other hand, the optimal algorithm is necessary to find the optimal number and location of wind turbines. Many non-conventional algorithms have been applied to extract maximum energy output corresponding to the optimization layout with regard to wind energy exploitation. These non-conventional algorithms are genetic algorithms (GA) [7], Monte Carlo simulations (MCs) [8], biogeography-based optimization [9], particle swarm optimization (PSO) [10] and derivative algorithms [11]. Of these optimization algorithms, the PSO has favorable search ability, fast convergence and no complicated evolutionary operators, but a derivative algorithm, such as improved particle swarm optimization (IPSO) has more rapid convergence speed compared to PSO [12]. By considering these two factors, many studies have been carried out to determine the problem with the WFLO. Peng et al. developed a PSO with multiple adaptive methods, based on the Jensen model, to find an optimal layout, which outperformed the baseline layout of a reference wind farm by increasing the energy yield by 3.84% under constant wind speed and variable wind direction [13]. Leandro et al. presented an approach expected to solve the problem of WFLO based on Gaussian wake model and the GA. Their results showed that there was a small improvement under a more complex wind scenario, in which variable wind speed and wind direction were defined [14]. From the existing approaches aimed at turbine layout optimization and application, the layout optimization can produce electrical energy at a lower cost and a higher efficiency. However, these studies have only taken the wake loss model and optimization algorithm into consideration, with a fixed design of the wind turbine. Thus, it may be beneficial to minimize the COE while simultaneously optimizing the wind turbines and their layout.

The wind energy extracted from the wind by a wind turbine is affected by the design parameters of the wind turbine. Recently, researchers have shown great attention to the WTDO, studying three approaches. One approach is to use optimum control algorithms in which Lidar-enhanced control [15] and model predictive control methods [16] are proposed for the torque system, and one-step model predictive control [17] and multi-step model predictive control methods [18] are proposed for the yaw system. Another approach is to optimize the blade shape, such as by an adaptive blade concept for large-scale turbines [19], and the lifting surface method, for airfoils aerodynamic shape optimization [20], so that the wind turbine can gain high energy harvesting efficiency [21]. Nevertheless, the optimization, in terms of the control algorithm and the blade shape, only contributes in some small way to the turbine design. By comparison, the last approach, namely, design optimization may achieve a low COE in an effective way, which involves the most important parameters of the overall design. The dominant methods for designing a satisfactory turbine with low COE require suitable physical and operational parameters, which are related to the wind resource at the selected site but have

rarely been studied. In Reference [22], the authors presented a framework for the site-specific design optimization of a horizontal-axis onshore wind turbine, in which the blade number, rotor diameter, tower height, rotor rotational speed, rated wind speed, and rated power were optimized to match the wind condition described by the Weibull distribution and parameters. Mirghaed et al. [23] developed an iterative approach to optimize a single turbine with minimum COE, in which the capital cost was a function of all turbine components, such as rotor diameter, hub height and rated power. In the study, it was found that the onshore turbines with capacities of about 1–2 MW lowered their COE by about 45–75 \$/MWh. In Reference [24], Luo et al. proposed a mathematical approach to minimize the COE of onshore turbines, in which the COE model was expressed as a function of rated power and rated wind speed. The above references have shown that the site-specific turbine design can achieve a low COE for onshore turbines, but studies of offshore wind turbines are lacking. Furthermore, the WTDO was only performed on an individual wind turbine rather than considering the whole wind farm, thus the achieved results may be unrealistic.

Currently, offshore wind turbines are designed to fit the large-size trend of high capacity and long blades and, thus, the issue of the high cost of energy is increasingly prominent. This paper aims to obtain the parameters of a cost-effective offshore wind farm. That is, a wind farm with a minimum COE. With regards to the literature, the contributions of this paper are summarized as follows. Firstly, this was the first study to address the COE optimization of wind farms by simultaneously optimizing the design parameters and the layout of wind turbines. Secondly, it established a mathematical description of the COE as a function of two design parameters of wind turbines and their layout, which can be extended to include more design variables. Thirdly, it proposed a composite optimization approach comprising an iterative algorithm and an improved particle swarm optimization (IPSO). As the concerned optimization issue involves two types of design variables, turbine design parameters and turbine layout, and the latter variable depends to some extent on the former, a single optimization approach may not be efficient to solve the issue. In the proposed approach, the iterative algorithm was the main optimization loop used to find the optimal wind turbine parameters, while the improved particle swarm optimization was a sub-optimization loop used to help the construction of the optimized layout. By doing so, the optimal solution could be conveniently determined. Finally, the utilization of the proposed approach was illustrated through three real offshore wind sites, which can be used as references for offshore wind farm designers.

The remaining sections are organized as follows: The COE model of offshore wind farms is discussed in Section 2, and Section 3 presents the method for optimizing COE by selecting the optimal wind speed, rotor diameter and the turbine layout. The case studies are described in Section 4 and, finally, Section 5 concludes the study.

2. Proposed Energy Cost Model for Offshore Wind Farms

The proposed COE of offshore wind farms relates to two factors: the total annual energy production (AEP_{total}) and the total annual cost ($Cost_{total}$), and is defined as follows:

$$COE = \frac{Cost_{total}}{AEP_{total}}, \quad (1)$$

where $Cost_{total} = \sum_i^N Cost_i$ and $AEP_{total} = \sum_i^N AEP_i$. $Cost_i$ and AEP_i represent the production cost and annual energy production of the individual wind turbine i , respectively. N is the number of wind turbines installed on the wind farm.

2.1. Annual Production Cost

On the offshore wind farm, two types of support platforms were applied, namely, the bottom-fixed platform and floating platform. Usually, the bottom-fixed platform is installed when the offshore wind farm is near the coastline, namely, the shallow-water sea, while the floating platform is employed

on sites far from the coastline or beyond, namely, the deep-water sea. As the cost is a key factor in determining the COE, the detailed cost model of the bottom-fixed offshore wind turbine developed by the National Renewable Energy Laboratory (NREL) was utilized and is expressed as [25]:

$$Cost_i = FCR \times ICC_i + AOE_i, \tag{2}$$

where $Cost_i$ is the total cost of turbine i , ICC_i is the initial capital cost, and AOE_i is the annual operating expense. FCR is the fixed charge rate, which is set to 0.1158 per year [25].

In the NREL cost model, the cost data of turbine components was available for different years. For the purpose of consistency, all cost data were converted to 2002 dollars before the cost and scaling factors were developed. ICC_i consists of the turbine system cost and the support platform station cost. The detailed costs are listed below.

(1) The turbine system cost.

The turbine system is divided into four main subsystems, the mechanical system (such as blade, gearbox and so on), electrical system (including generator, power converter and electrical connection), control system (safety system, yaw control, torque control and pitch control), and auxiliary system, such as hydraulic cooling equipment, hub and tower. Since the number of blades is three, the turbine system cost, ICC_{turb} , is given by:

$$ICC_{turb} = 209.526P_r + 16.45P_r^{1.249} + 206.69R + 11.9174(2R)^{1.953} - 0.01069(2R)^{2.5} + 11.4354R^{2.5025} + 2.00617R^{2.53} + 0.48017(2R)^{2.6578} + 0.01(2R)^{2.887} + 0.0678(2R)^{2.964} + 1.67458R^3 + 0.00432(2R)^{3.5} + 0.59595\pi R^2 H + 73990.5 \tag{3}$$

According to Equation (3), the value of ICC_{turb} is determined by the parameters of the wind turbine corresponding to the rated power, rotor radius and hub height. So ICC_{turb} can be expressed as a function of P_r , R and H , namely, $ICC_{turb} = f_1(P_r, R, H)$.

(2) The support platform station cost.

The ICC_{BoP} involves the cost of infrastructure and offshore engineering, and the detailed mathematical models are shown in Reference [25]. According to the report of NERL, the ICC_{BoP} can be summarized as

$$ICC_{BoP} = 0.311325ICC_{turb} + 755.402P_r + 1.62843 \times 10^{-5}P_r^3 - 0.038625P_r^2 + 56.341P_r + 58710 \tag{4}$$

From Equation (4), the ICC_{BoP} is determined by the turbine system cost and rated power, and ICC_{BoP} can be expressed as $ICC_{BoP} = 0.311325f_1(P_r, R, H) + f_2(P_r)$.

(3) The annual operating expense.

The annual operating expense AOE consists of the land lease, levelized operation and maintenance (OM), and the levelized replacement costs. Its mathematical formula is

$$AOE_i = 17P_r + 0.02108AEP_i \tag{5}$$

According to Equation (5), the AOE_i is determined by the rated power and the annual energy production. So, referring to Equations (2)–(5), the wind turbine i cost can be expressed as

$$Cost_i = f_{costi}(P_r, R, H, AEP) = 0.151851435f_1(P_r, R, H) + 0.1158f_2(P_r) + 17P_r + 0.02108AEP_i \tag{6}$$

In the above equation, Equation (6), $Cost_i$ was estimated based on the empirical model, which is related to the rated power, rotor radius, tower height, and AEP of the wind turbine i . Since the AEP of the wind farm is determined by the parameters and layout of wind turbines, it is possible to minimize the cost of the wind farm by designing the appropriate wind turbine parameters and their layout.

2.2. Annual Energy Production

Normally, the AEP_i of the offshore turbines is estimated based on the Weibull probability distributions of the wind statistics, a standardized power curve, a physical description of the turbine and physical constants. Although this method can effectively estimate the AEP of single wind turbines, it was simplified in the present context to ignore the wake effects and wind turbine layout when applied to estimate the AEP_{total} of the whole offshore wind farm. So, in this paper, the existing AEP model is modified by taking wind turbine's wake effect and layout into consideration.

The AEP_i of a turbine can be given by the average power production, $P_{avg,i}$, of the wind turbine i during one hour and the total hours of one year:

$$AEP_i = 8760(1 - \zeta)P_{avg,i} \tag{7}$$

where ζ is the total power generation loss, including power converter loss, electrical grid loss, availability loss and so on. In this study, ζ is assumed to be a constant of 0.16 [26].

Meanwhile, the mean power production, $P_{avg,i}$, of a single wind turbine can be calculated as:

$$P_{avg,i} = \int_0^\infty P(v)f_i(v)dv, \tag{8}$$

where v is the wind speed, $P(v)$ denotes the power curve model as a function of the wind speed, and $f_i(v)$ is the Weibull distribution corresponding to the installation site, which is also as a function of the wind speed.

2.2.1. Power Curve Modeling of the Offshore Turbines

Figure 1 shows the four control regions in wind turbines based on wind speed. In Region 1, where the wind speed is below cut-in speed (v_c), the wind turbine is in standby mode. In Region 2, where the wind speed is between v_c and the rated speed (v_r), the turbine is able to generate partial power. In Region 3, where the wind speed is between v_r and the cut-off speed (v_f), the wind turbine is limited to the rated power. In Region 4, where the wind speed is above the v_f , the turbine is shut down or, better, set aside to avoid component over-loads. Thus, the power curve model can be expressed analytically as:

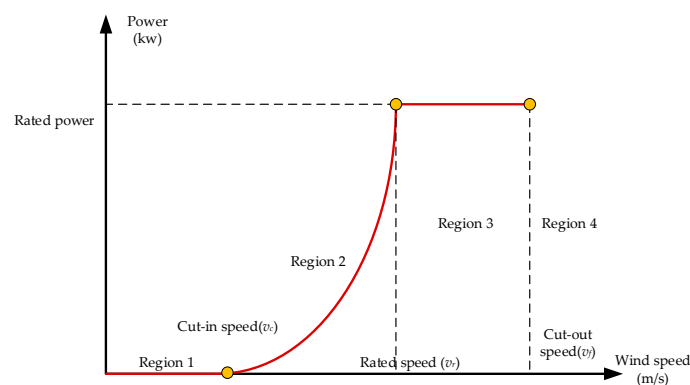


Figure 1. Four regions of the wind turbine power curve.

$$P(v) = \begin{cases} 0 & (v < v_c) \\ P_f(v) & (v_c \leq v \leq v_r) \\ P_r & (v_r \leq v \leq v_f) \\ 0 & (v_f < v) \end{cases} \tag{9}$$

where $P_f(v)$ is the active power when the wind passes through a wind turbine and is exploited by it. The mathematical formula of $P_f(v)$ is given by:

$$P_f(v) = \rho\pi R^2 C_p v^3 / 2, \tag{10}$$

where ρ and R denote the air density and the rotor radius, respectively; C_p denotes the coefficient of power that depends on the wind speed, which is assumed as constant and equal to 0.42 for simplicity [26]. Then, the turbine rated power P_r can be calculated as

$$P_r = \rho\pi R^2 C_p v_r^3 / 2 \tag{11}$$

2.2.2. Weibull Probability Density Distribution of Offshore Wind Statistics

In this study, the Weibull probability density function $f_i(v)$ was employed to represent the offshore wind statistics of the installation site, which depended on the Weibull scale and the shape parameters k_i and c_i that determined the shape and intensity of the wind during one year on a site [27].

$$f_i(v) = (k_i / c_i)(v / c_i)^{k_i-1} e^{-(v/c_i)^{k_i}}, \tag{12}$$

where c_i and k_i denote the Weibull scale and the shape parameters in the location of wind turbine i , respectively.

Assuming that the shape factor k_0 at the reference hub height H_0 and the annual mean wind speed v_{mi} are known constants for the offshore wind farm, the scale factor c_0 can be calculated as:

$$c_0 = v_{mi} / \Gamma(1 + 1/k_0), \tag{13}$$

where Γ is the gamma function.

The wind speed becomes stronger as the altitude, i.e., the distance from the ground, increases. Based on the relationship between the wind speed and the altitude, the shape factor k and scale factor c at the turbine i hub height H are obtained by:

$$c_i = c_0(H/H_0)^\alpha \tag{14}$$

$$k_i = k_0[1 - 0.088 \ln(H_0/10)] / [1 - 0.088 \ln(H/10)], \tag{15}$$

where, α is the Hellmann exponent, which depends on surface properties of the wind field. The typical value of α is 0.1 over water and 0.14 over land [27].

When the Weibull probability distribution of a single wind turbine in its erected site is mainly determined by the wind characteristics of the wind farm, it is also influenced by the wake effects of the wind farm. Generally, the wake effect leads to a reduced wind speed that is faced by the downwind turbines. In this study, the Jensen wake loss model was adopted for its low computational cost. With the Jensen wake loss model, the wind velocity deficit behind an upstream wind turbine is calculated by the following equation:

$$v_i = v_m [1 - (1 - \sqrt{1 - C_t})(\frac{D}{D_w})^2], \tag{16}$$

where v_m is the mean wind speed and C_t is the axial induction factor, which is set to 0.88 for simplify [28]. D and D_w denote the wind turbine rotor diameter and wake diameter, respectively. The equation of D_w is given by:

$$D_w = D + 2k_w x, \tag{17}$$

where x is the downstream distance from the wind turbine and k_w presents the wake decay coefficient. In this study k_w was set at 0.04 [28].

In the actual offshore wind farm, a downstream wind turbine i was affected by multiple wakes of upstream wind turbines. Supposing that the number of upstream wind turbines is M , the wind velocity of wind turbine i can be represented as follows:

$$v_{mi} = v_m \left[1 - (1 - \sqrt{1 - C_t}) \sqrt{\sum_{j=1}^M \frac{1}{(1 + 2k_w \frac{x_{ij}}{D})}} \right], \tag{18}$$

where x_{ij} denotes the horizontal distance between upstream wind turbine j and downstream wind turbine i .

Based on Equations (12)–(18), the shape factor $k_i(H, k_0)$ can be expressed as a function of hub height and k_0 , and the scale factor $c_i(H, k_0, v_m)$ depends on the hub height, k_0 , and mean wind speed v_{mi} . From Reference (18), it was gathered that the wind speed extracted by turbine i is a function of the distance x between the installation sites of two turbines and the rotor diameter D or rotor radius, so the scale factor c_i can be expressed as $c_i(H, k_0, v_m, R, x)$.

Therefore, based on Equations (7)–(18), the AEP of the offshore turbines was expressed as a function of the wind statistics factors v_m, k_0 , and α , the turbine characteristics parameters v_c, v_r, v_f and R and layout factor x , formulated by

$$AEP_i = f_{AEP_i}(R, H, v_r, v_c, v_f, v_m, k_0, \alpha, x) \tag{19}$$

2.3. Energy Cost Model of Offshore Wind Farms

By replacing Equation (1) with Equations (6) and (19), the COE can be written as

$$COE = \frac{Cost_{total}}{AEP_{total}} = \frac{\sum f_{cost_i}(P_r, R, H, f_{AEP_i}(R, H, v_r, v_c, v_f, v_m, k_0, \alpha, x))}{\sum f_{AEP_i}(R, H, v_r, v_c, v_f, v_m, k_0, \alpha, x)} \tag{20}$$

According to the European Wind Energy Association, there is a relationship between the hub height and the turbine rotor radius, which is expressed by Reference [29] as

$$H = 2.7936 \times (2R)^{0.7633} \tag{21}$$

Substituting Equations (11) and (21) into Equation (20), P_r can be replaced with a function of R and H , while H is replaced with R . Thus, the COE model of the offshore wind farm is formulated as

$$COE = \frac{\sum f_{cost_i}(R, f_{AEP_i}(R, v_r, v_c, v_f, v_m, k_0, \alpha, x))}{\sum f_{AEP_i}(R, v_r, v_c, v_f, v_m, k_0, \alpha, x)} \tag{22}$$

In Equation (22), the COE model of offshore wind farms was formulated as a nonlinear function in which the rated wind speed, the rotor radius, and the spacing among the turbines were the design parameters, i.e., the target parameters, the cut-in and cut-out wind speeds were typically known constant parameters, and the wind statistics of the offshore windfarm were the mean wind speed, the shape factor, and the Hellmann exponent. Thus, the final expression of COE after modifications is

$$COE = \frac{\sum f_{cost_i}(R, f_{AEP_i}(R, v_r, v_m, k_0, \alpha, x))}{\sum f_{AEP_i}(R, v_r, v_m, k_0, \alpha, x)} \tag{23}$$

3. Energy Cost Optimization for Offshore Wind Farms

Based on Equation (23), the minimization of the COE of the offshore wind farms can be fulfilled by optimizing the three design parameters: the rated wind speed, the rotor radius and x . As the objective

is to minimize the COE, when considering the practical constraints, the objective function and the constraint can be expressed as:

$$COE^{min}(R, v_r, x) = \min(COE(R, v_r, x)) \tag{24}$$

$$s.t. \{ R^{min} \leq R \leq R^{max}, v_r^{min} \leq v_r \leq v_r^{max}, x^{min} \leq x \leq x^{max} \}$$

where, R^{min} and R^{max} are the minimum and maximum values of the rotor radius, v_r^{min} and v_r^{max} are the minimum and maximum values of the rated wind speed, x^{min} and x^{max} are the minimum and maximum distances between two wind turbines, respectively.

In the following sections, the method to minimize the cost of energy of the offshore wind farm is elaborated, the optimization results are presented, and discussions explain the obtained optimization results.

3.1. Optimization Method

In order to minimize the COE, a composite optimization approach was proposed, comprising an IPSO and an iterative algorithm. The first was applied to help the construction of the optimized layout, while the second was used to find the optimal parameters of wind turbines that give the minimum COE. The theory and optimization procedure are presented in the following section.

3.1.1. Improved Particle Swarm Optimization

Particle swarm optimization (PSO), developed by Eberhart and Kennedy, is a population-based stochastic optimization technique and it is recognized as a simple concept algorithm, with easy coding implementation, robustness to control parameters and computational efficiency. When compared with the PSO, the IPSO algorithm has improved the convergence performance [12]. The IPSO equations are given as:

$$v_{id}^{new} = w \cdot v_{id}^{old} + c_1 \cdot r_1 \cdot (p_{id} - x_{id}^{old}) + c_2 \cdot r_2 \cdot (p_{gd} - x_{id}^{old}) \text{ and} \tag{25}$$

$$x_{id}^{new} = x_{id}^{old} + v_{id}^{new} \quad 1 \leq i \leq n, 1 \leq d \leq M, \tag{26}$$

where v_{id} , x_{id} , p_{gd} and p_{id} denote the velocity vector, the position of the i th particle, the global best position and individual best position, respectively. c_1 and c_2 are the positive acceleration constants and the condition $c_1 + c_2 \leq 4$ is satisfied. $r_{1,2}$ is a random number between 0 and 1. n is the total number of particles and M is the dimension of searching space. In order to avoid going beyond the searching space, the velocity, v_{id} , needs to be set into a limited range, namely $v_{min} \leq v_{id} \leq v_{max}$. w is the inertial weight in this study and its expression is as follows:

$$w = \left(\frac{w_{max}}{w_{min}} \right)^{\frac{1}{1+10 \frac{t}{T}}}, \tag{27}$$

where t is the current iteration number, and T is the total iteration number. w_{max} and w_{min} are maximum and minimum inertial weights, set to 0.9 and 0.4 in this study, respectively.

3.1.2. Optimization Procedure

As regards the model to minimize the COE model, the composite optimization algorithm is designed into two parts: One is the main optimization algorithm, which uses the iterative algorithm to obtain the optimally designed parameters of the wind turbines, while the other is the sub-optimization algorithm, which employs the IPSO algorithm to obtain an optimal turbine layout by comparing the values of the objective function. The main flow chart of the developed algorithm is presented in Figure 2, and the implemented procedures comprise the following two loops.

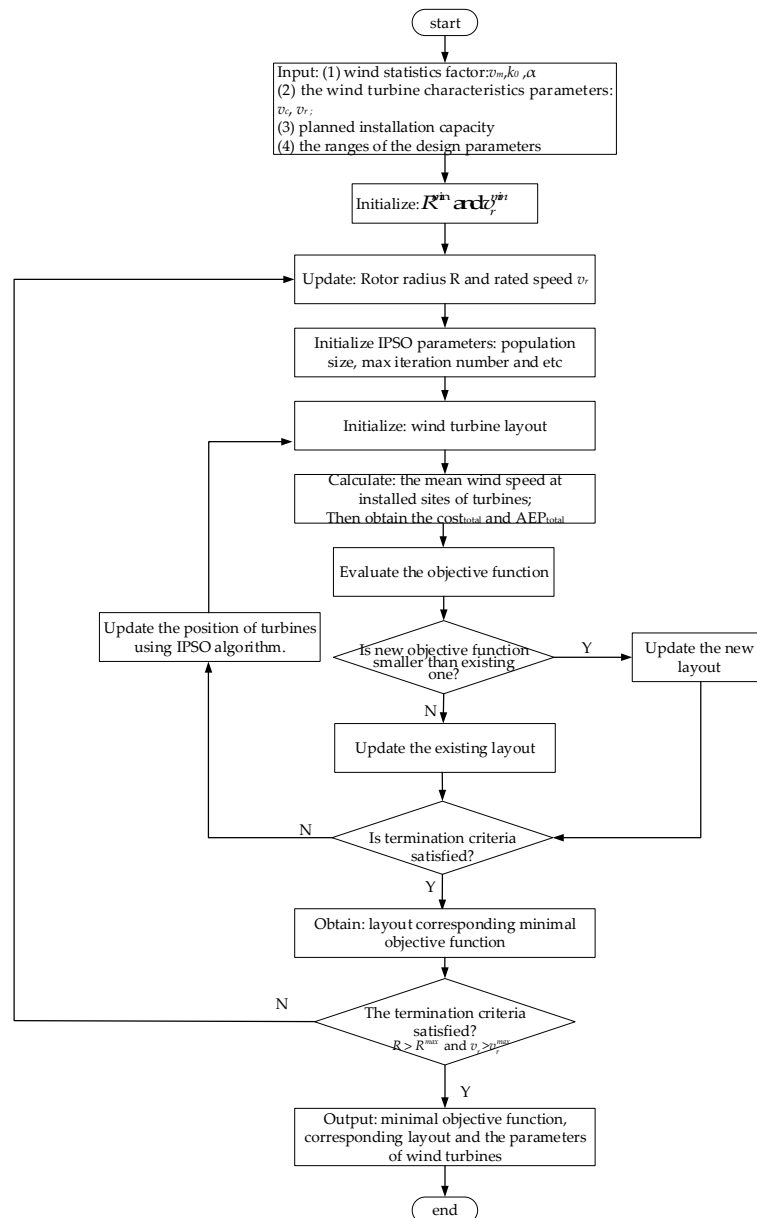


Figure 2. Flow charts of the proposed COE minimization approach.

(1) The main optimization loop.

- Step 1: Initialize the wind statistics of the offshore windfarm, v_m , k_0 and α ;
- Step 2: Define the ranges of the design parameters v_r , R and initialize the minimum design parameters.
- Step 3: Update the design parameters through their own iterative intervals.
- Step 4: Turn to the IPSO algorithm and obtain the optimal turbine layout and value of the objective function (COE).
- Step 5: Repeat step 3 until all design parameters sets of v_r and R have been evaluated;
- Step 6: Output, with minimal objective function, the corresponding design parameters and wind turbine layout.

(2) The sub-optimization loop.

- Step 1: Input the wind statistics of the offshore wind farm, v_m, k_0 and α . Input the wind turbine characteristics parameters, v_c, v_r, v_f , and R and input the planned installation capacity. Define the grid size of the offshore wind farm.
- Step 2: Initialize the IPSO parameters $c_1, c_2, n, w_{max}, w_{min}, t, T, v_{id}, x_{id}, v_{max}$ and v_{min} . Initialize the wind turbine layout: assume the wind turbines are installed in the grid-center and generate a set of numbers which represent the wind turbine layout according to the grids.
- Step 3: According to Equations (16)–(18), calculate the mean wind speed at the installation sites of turbines and then obtain the $cost_{total}$ and AEP_{total} .
- Step 4: Evaluate the objective function via the question, “Is the new result of the objective function smaller than the existing one?” Update the layout corresponding to the smaller one.
- Step 5: Determine whether the procedure termination condition has been met. If yes, turn to Step 8; if no, turn to Step 6.
- Step 6: Update the wind turbine layout by IPSO until there is no duplicate value.
- Step 7: Repeat Step 3 until the procedure termination condition is satisfied.
- Step 8: Output the minimal objective function and the corresponding layout.

4. Method Application and Resulting Discussion

To show how to minimize the cost of energy for the offshore wind farms by using the proposed step by step optimization approach, case studies were conducted. Since the proposed COE model depended on the wind statistics of the offshore wind farm, the real wind information from some offshore wind farms was used for this study.

4.1. Parameter Settings

In this study, the capacity of planned–installed wind farms was assumed to be 60 MW. The parameters of the wind turbines and the proposed COE are summarized in Table 1, in which the rated wind speed is in the range 10–16 m/s with a step of 1 m/s and the rotor radius is in the range 30–70 m with a step of 5 m. Assuming a regular grid for the offshore wind farm, the grid size was 10×10 , and the interval between the two wind turbines was $6D$ (D denotes the rotor diameter).

Table 1. Parameters used in the proposed COE minimization method.

Parameter	Values or Ranges
H_0	10 m
α	0.1
ρ	1.225 kg/m ³
R	[30, 70] with a step of 5 m
v_r	[10, 16] with a step of 1 m/s
v_c	3 m/s
v_f	25 m/s
$C_{p,eq}$	0.42

For the IPSO algorithm, the algorithm convergence speed relied largely on the initial values of the particles at the first iteration. Meanwhile, the two important parameters, including the population size and the maximum iteration number, also significantly influenced the optimal results. With a certain set of initial values of the particles, the selected objective function value was more optimal, that is, more significant, when the population size and the maximum iteration number was bigger. However, more computation time is required. In this study, the population size and the maximum iteration number of IPSO were set to 20 and 200, respectively. By doing so, the IPSO reached convergence and the computation time was about ten days for each case. The acceleration factors c_1 and c_2 were set as

1.49445. Then, the obtained position layout was applied to analyze the developed COE. On the other hand, in order to analyze the relationship between the developed COE and the layout, the optimal wind turbine obtained by the developed COE and the actual installed wind turbines were taken into consideration for comparison.

4.2. Method Application in Three Cases

Three real installations were used as case studies: Newport nearshore windpark (NNW) wind site in the USA, Xiangshui intertidal Pilot project (XIPP) offshore wind farm in China, and Rønland offshore wind farm in Denmark. The wind statistical data of the three wind sites is given in References [30–32], respectively, and the Weibull distribution parameters of wind speed are summarized in Table 2. The wind direction is assumed to be constant. The distribution curves of the wind speed are plotted in Figure 3.

Table 2. Wind statistic data of three offshore wind farms.

Offshore Wind Farm	Mean Wind Speed (m/s)	Shape Factor (k_0)	Scale Factor (c_0 , m/s)
NNW, USA	8.23	2.0	9.29
XIPP, China	6.84	2.0	7.83
Rønland, Denmark	10.2	2.0	11.51

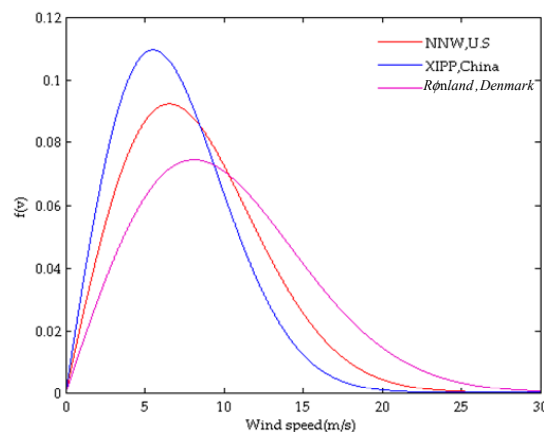


Figure 3. Weibull probability distribution functions of three cases at reference hub height H_0 .

Case 1: NNW offshore wind farm, USA, is located at latitude 39.201° and longitude -75.241° .

At this wind farm, the mean wind speed was 8.23 m/s and the shape factor k_0 of the Weibull distribution function was 2.0. Based on the presented cost of energy and the optimization approach, the results about the relationships among the rated speed, rotor radius and COE were obtained and are shown in Figure 4a,b. As seen in Figure 4, the results show that the wind farm has a minimum COE of 0.077 \$/kWh for turbines with a rated speed of 11 m/s and a rotor radius of 50 m. By calculation, the rated power of the turbine is about 2.7 MW, and the hub height is 95.23 m. The actual wind turbines installed in NNW wind farm include the SWT-3.6-120 for which the main parameters are given in Table 3. It is shown that the optimization results are close to the values of the actual wind turbine. However, compared to the wind turbine with the minimum COE, the actual wind turbine has a higher speed and rotor radius.

Table 3. Main parameters of the wind turbine installed in NNW, USA.

Types	Cut-in Speed (m/s)	Cut-off Speed m/s	Speed m/s	Power (MW)	Hub Height (m)	Rotor Radius (m)
SWT-3.6-120 (Siemens)	3–5	25	12–13	3.6	90	60

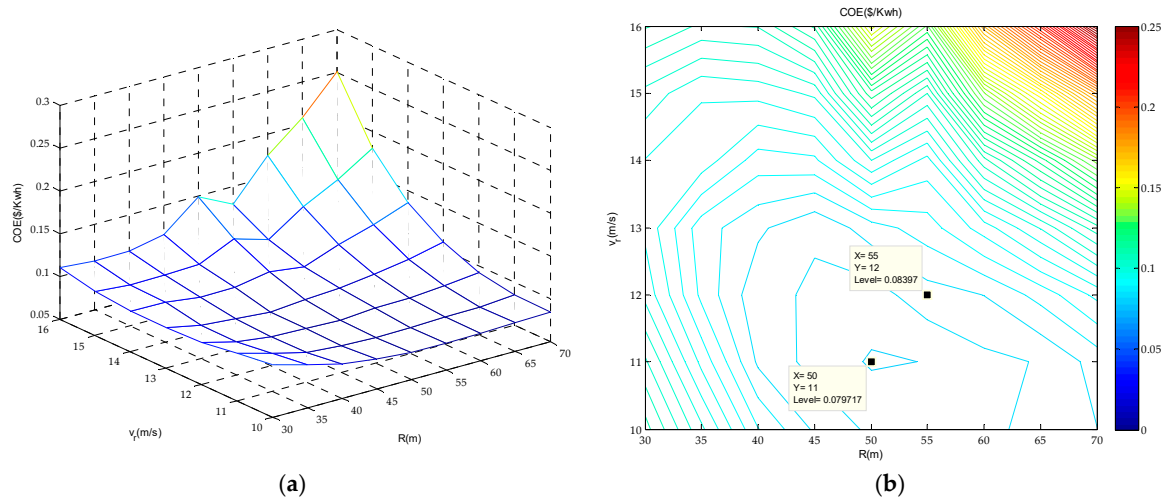


Figure 4. The relationship between the speed, rotor radius and COE: (a) 3D graphic and (b) contour map.

In order to prove the effectiveness of the proposed COE method, an analytical comparison about the minimum COE of an optimal turbine and SWT-3.6-120 was performed. It considered the optimal wind turbine layout obtained by the IPSO algorithm. As the planned–installed capacity of offshore wind farms is 60 MW, 17 wind turbines were expected to be installed, $N = 17$. The optimization results and the optimal layout obtained by the IPSO algorithm are shown in Figure 5a,b, respectively. In Figure 5a, when the value of the minimum COE of the SWT-3.6-120 ($COE_{min} = 0.0787$ \$/kWh) is higher than the COE value of the optimal wind turbine, of which the value is 0.0774 \$/kWh, the minimum COE of the actual wind turbine is very close to the minimum COE value of the optimal wind turbine. In Figure 5b, as expected, the layout of the wind turbines has a tendency to locate the turbines in the outermost zone of the grid and the distance between two wind turbines is higher in the wind direction. As such, the layout of the wind turbines can reduce the influence of the wake-effect and, accordingly, the effectiveness of the layout optimization is confirmed. The IPSO was used to search for the optimal layout of wind turbines and, thus, the convergence of the IPSO could be judged by checking the final layout of the wind turbines. Since the optimized layout in Figure 5b is consistent with the expected results, it can be determined that the IPSO converged after 200 iterations.

Case 2: The XIPP offshore wind farm in China is located at latitude 34.464° and longitude 119.871° .

At this wind farm, the mean wind speed was 6.94 m/s and the shape factor, k_0 , of the Weibull distribution function was equal to 2.0. Based on the cost of energy presented and the two optimization methods, the results about the relationships between the speed, rotor radius and COE were obtained, as shown in Figure 6a,b. The results show that the wind farm has a minimum COE of 0.089 \$/kWh at a rated speed of 10 m/s and a rotor radius of 60 m. The power of the turbine was about 2.9 MW and the hub height was 109.5 m. The actual wind turbines installed in the XIPP offshore wind farm included the GW 109/2500 (Goldwind, Beijing, China) and the W2000/93 (Sewind, Shanghai, China). The main parameters of these wind turbines are detailed in Table 4. Compared with the optimal turbine, the actual wind turbines had slightly higher speeds and lower rotor radii. When comparing the two actual turbines, the GW 109/2500 was the optimal turbine due to its lower COE.

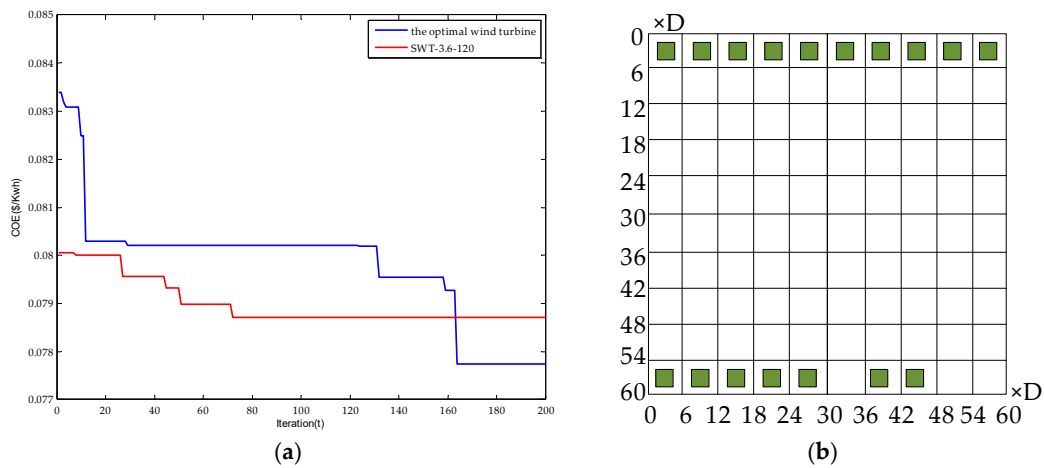


Figure 5. The results of the objective function (COE) and optimal layout: (a) result of objective function and (b) optimal layout.

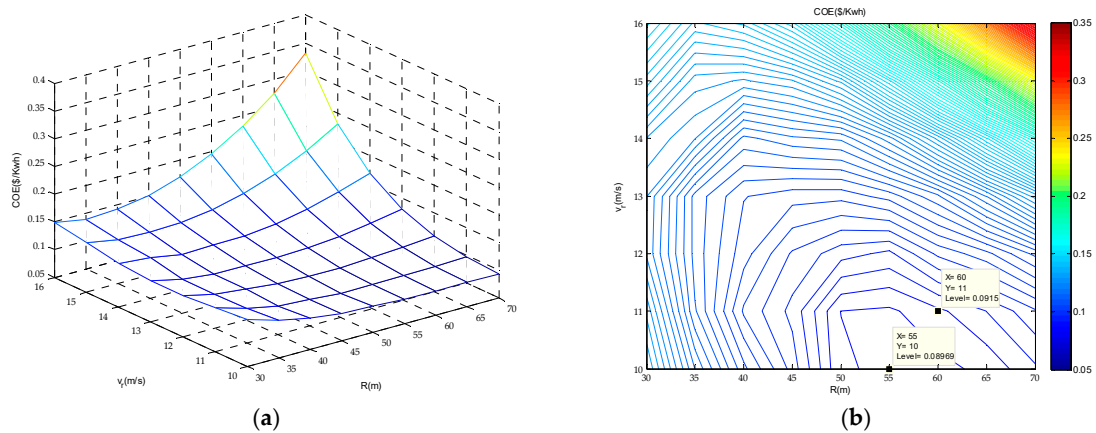


Figure 6. The relationship between the speed, rotor radius and COE at XIPP, China: (a) 3D graphic and (b) contour map.

Table 4. Main parameters of the wind turbine installed in XIPP, China.

Types	Cut-in Speed (m/s)	Cut-off Speed (m/s)	Speed (m/s)	Power (MW)	Hub Height (m)	Rotor Radius (m)
GW 109/2500 (Goldwind)	3	25	10.1	2.5	80	54.5
W2000/93 (Sewind)	3	25	10.8	2.0	80–90	46.5

The analytical comparison of the minimum COE of the optimal turbine, GW 109/2500 and W2000/93 was adopted in terms of the optimal wind turbine layout obtained by the IPSO algorithm. As the planned-installed capacity of offshore wind farms was 60 MW, 24 GW 109/2500 wind turbines were expected to be installed, $N = 24$. The number of W2000/93 wind turbine was 30. These optimization results and the optimal layouts of the two wind turbines obtained by the IPSO algorithm are shown in Figure 7. It can be seen from Figure 7a that the GW 109/2500 had a smaller COE than the W2000/93. The former had the same result as that of the developed optimization method. In Figure 7b,c, the layouts of the wind turbines are arranged into three rows: Two rows are located in the outermost zone of the grid and one row is located in the medial grid. In this way, the spacing between the two wind turbines is biggest in the wind direction. Consequently, the influence of the wake-effect on the energy production was reduced and, again, the effectiveness of the layout optimization was confirmed.

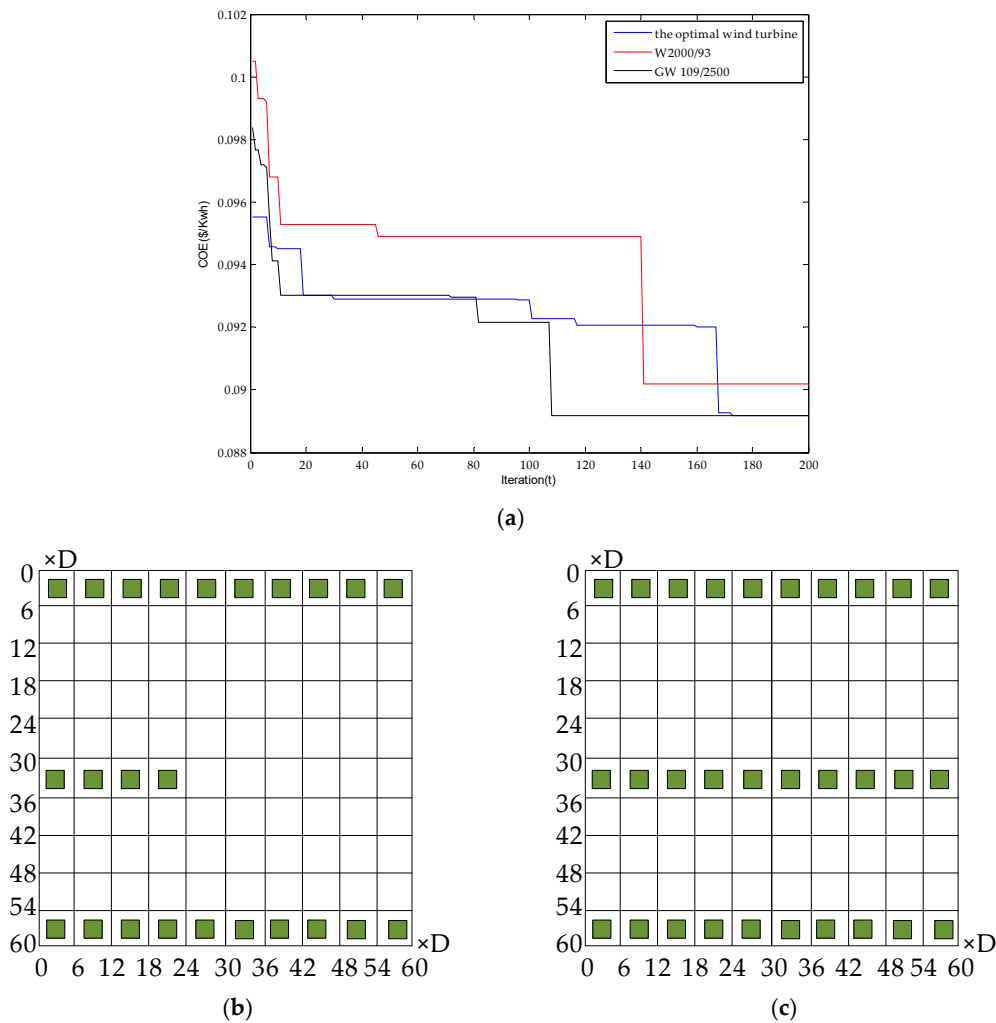


Figure 7. The results of the objective function (COE) and optimal layout: (a) results of objective function, (b) optimal layout of GW109/2500, and (c) optimal layout of W2000/93.

Case 3: The *Rønland* offshore wind farm, Denmark, is located at latitude 56.662° and longitude 8.221° .

At this wind farm, the mean wind speed was about 10.20 m/s and the shape factor k_0 of the Weibull distribution function was equal to 2.0. The optimization results are shown in Figure 8a,b. The results showed that the wind farm had a minimum COE of 0.0695 \$/kWh at a speed of 12 m/s and a rotor radius of 40 m. The power of the turbine was about 2.23 MW and the hub height was 80.26 m. The two actual wind turbines installed at the *Rønland* wind farm included the SWT-2.3-93 (Sewind) and the Vestas v80-2000. The main parameters of the wind turbines are detailed in Table 5. It shows that the Vestas v80-2000 has lower speed, lower power and the same rotor radius, and the SWT-2.3-93 has lower speed and higher rotor radius compared to the optimal turbine. Besides, from the Figure 8b, the minimum COE of the two actual wind turbines was approximately the same.

Table 5. Main parameters of the wind turbine installed in *Rønland*, Denmark.

Types	Cut-in Speed (m/s)	Cut-off Speed (m/s)	Speed (m/s)	Power (mw)	Hub Height (m)	Rotor Radius (m)
Swt-2.3-93 (Siemens)	3	25	11.0	2.3	80	46.5
Vestas v80-2000	3–5	25	11.5	2.0	60–101	40

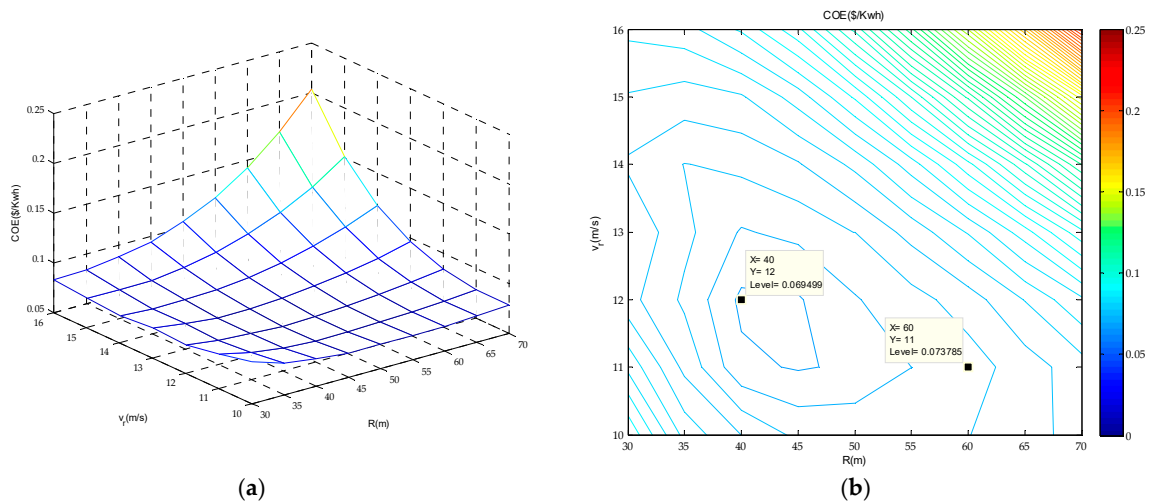


Figure 8. The relationship between the speed, rotor radius and COE at the *Rønland* offshore wind farm, Denmark: (a) 3D graphic and (b) contour map.

In order to prove the effectiveness of the proposed COE method, an analytical comparison of the minimum COE of the optimal turbines, SWT-2.3-93 and Vestas v80-2.0 MW was proposed. This considered the optimal wind turbine layout obtained by IPSO algorithm. According to the planned–installed capacity of the offshore wind farm, 27 wind turbines were expected to be installed, $N = 27$. Analogously, the planned–installed number of Vestas v80 was 30. The optimization results and the optimal layouts obtained by the IPSO algorithm are shown in Figure 9. It can be seen from Figure 9a that when the Vestas v80-2.0 MW had a COE slightly smaller than the SWT-2.3-93, both of their COE were higher than the optimization result. Figure 9b,c shows the optimal layouts of the wind farm with the two actual wind turbines. Similar to Figure 7b,c, there are three rows of the layout of the wind turbines, among which two rows are located in the outermost zone of the grid, while one row is located in the medial grid. The biggest spacing was maintained between two wind turbines in the wind direction and, thus, the influence of the wake-effect on the energy production was most diminished.

4.3. Discussion

In order to check the advantages of the proposed optimization method, the differences between the optimal COE of the three optimized wind farms and the actual wind turbines were calculated and are shown in Table 6. The results show that these differences are positive and their values are in a range of 0–0.001 \$/kWh, and the reduced ratio of the COE is in the range 0–1.27%. Thus, it seems that the actual wind turbines may have been optimally designed before being installed in the offshore wind farms [33,34]. On the other hand, the positive differences mean that it is necessary to simultaneously optimize the wind turbines and their layout to achieve the minimal energy cost of the offshore wind farms.

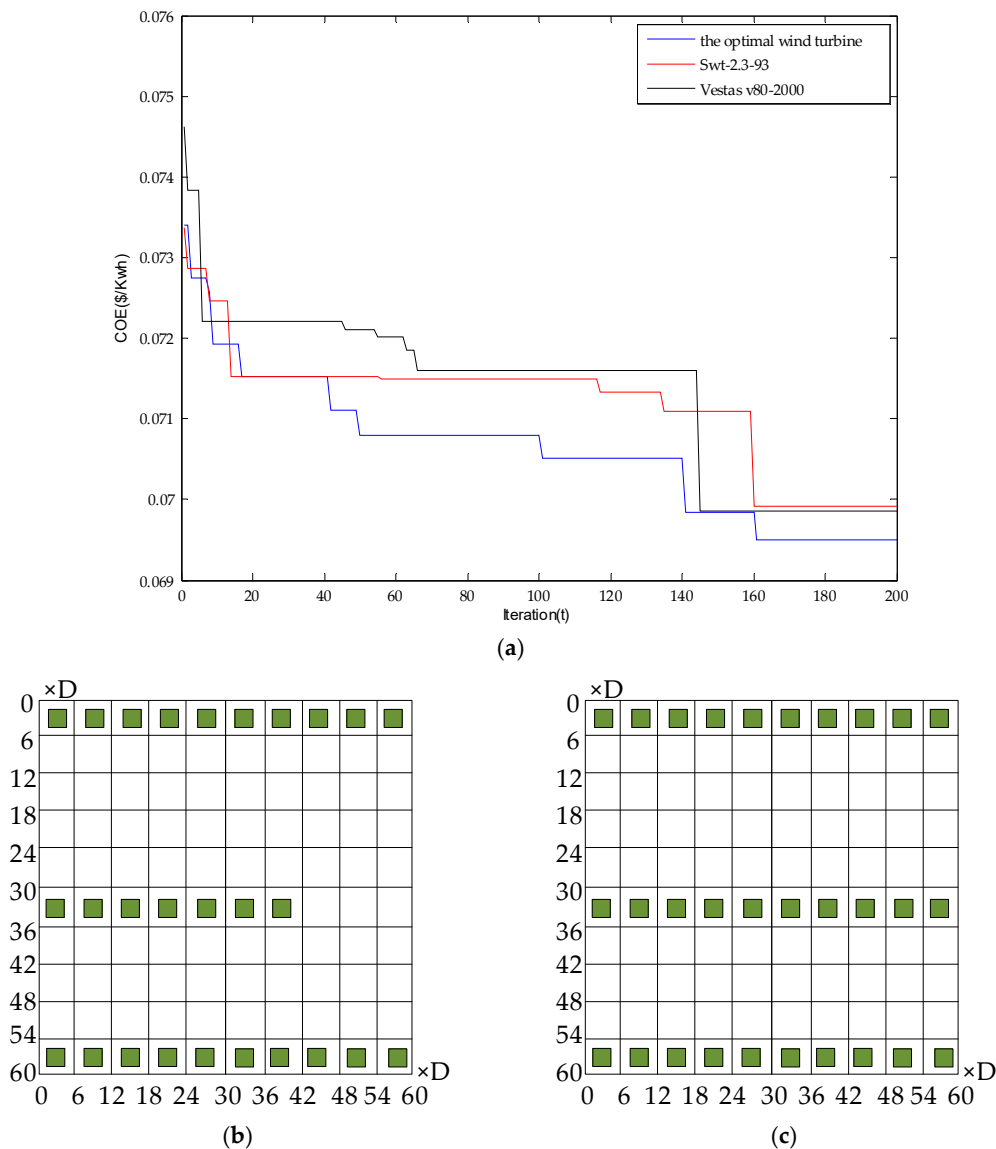


Figure 9. The results of the objective function (COE) and optimal layout: (a) results of objective function, (b) optimal layout of Swt-2.3-93, and (c) optimal layout of Vestas v80-2.0MW.

Table 6. The results of minimum COE corresponding to the optimal layout.

Wind Farm	NNW, USA		XIPP, China		Rϕnland, Demark			
Annual mean wind speed (m/s)	8.23		6.94		10.2			
Type	The optimal one	SWT-3.6-120	The optimal one	GW 109/2500	W2000/93	The optimal one	Swt-2.3	Veatas v80
COE _{min} (\$/kWh)	0.0777	0.0787	0.0892	0.0892	0.0902	0.0695	0.0699	0.0698
Difference	-	0.001	-	0	0.001	-	0.0004	0.0003

In order to check the optimization rules of the designed parameters of the wind turbines in the offshore wind farms, considering the optimal value of the COE varying in the range of 0.002 \$/kWh, the range of the optimally designed parameters are shown in Table 7. From Table 7, it is clear that when the mean wind speed is increased, the optimally designed rotors slightly decrease their size, while the rate wind speeds are higher. Although it seems contradictory to the current trend of offshore wind turbines towards having long blades, it is acceptable as the optimization results actually confirm the fact that the COE is more sensitive to the variation of the wind speed rather than the rotor radius. Furthermore, the final capacities of the optimally designed wind turbines are calculated by using the

optimal rotor radius and wind speed, and their results are 2.0–3.9, 2.4–4.5, and 1.7–5.6 MW for the annual mean wind speed with 6.94, 8.23, and 10.2 m/s, respectively. These results reveal that the wind farm with a high mean wind speed can have a wider range of the turbine capacities than one with a low wind speed. Thus, there is freedom for designers to design the offshore wind turbines, which can be seen as another advantage in the construction of wind farms at wind sites with rich wind resources, besides the favorable COE.

Table 7. The results of the optimum range of COE corresponding the wind turbine.

Wind Farm	NNW, USA	XIPP, China	Rϕnland, Demark
Annual mean wind speed (m/s)	8.23	6.94	10.2
Range of optimal COE	0.077–0.079	0.089–0.091	0.0699–0.072
Rotor radius (m)	45–65	50–65.5	40–60
Rated speed (m/s)	10–12	10–11.5	10.5–13
Rated power (MW)	2.4–4.5	2.0–3.9	1.7–5.6

Furthermore, by summarizing the optimal layouts of the three cases studied, it is clear that the results show a similar tendency, that the biggest spacing between two wind turbines is kept in the wind direction, which is consistent with the expected results. By doing so, the impact of the wake loss effect on the energy production was farthest and, accordingly, the results confirmed the usefulness of optimization in layout determination.

5. Conclusions and Future Work

This paper proposed a systematic optimization method to minimize the energy cost of offshore wind farms through a search for the optimal wind speed and rotor radius of individual turbines and the optimal turbine layout. To do this, the energy cost minimization problem was formulated and a composite optimization approach was used, as presented in this paper. The proposed method was applied to three case studies using real wind resources. The results showed that the energy cost was reduced by 0–1.27%, confirming the effectiveness of the conducted optimization. More importantly, exploring the obtained optimal results provided some deep insights into the optimization design of offshore wind farms, including that the energy cost of wind turbines is more sensitive to the variation of the wind speed than the rotor radius, and that wind sites with rich wind resources can have a wider range of turbine capacity than those with poor wind resources. In future work, more design parameters and new objective functions can be considered within the presented optimization framework. However, it is worth pointing out that the optimization algorithm and the proposed energy model may be improved to save time during the optimization procedure.

Author Contributions: All the author contributed to this work. X.Z. designed the methodology and wrote the original draft of the paper under the supervision of L.L. (Longfu Luo); D.S. provided the resources and revised the draft; W.T. helped write and review the draft; X.T. and L.L. (Li Li) contributed to the algorithm design, data collection, and visualization.

Acknowledgments: This work was supported in part by the National Natural Science Foundation of China, under Grant 61803393 and 51777217, and the project was funded by the China Postdoctoral Science Foundation, under Grant 2017M622605.

Conflicts of Interest: The authors declare no conflicts of interest.

References

1. Heptonstall, P.; Gross, R.; Greenacre, P.; Cockerill, T. The cost of offshore wind: Understanding the past and projecting the future. *Energy Policy* **2012**, *41*, 815–821. [[CrossRef](#)]
2. Sorensen, T.; Nielsen, P.; Thøgersen, M.L. Recalibrating wind turbine wake model parameters—Validating the wake model performance for large offshore wind farms. In Proceedings of the European Wind Energy conference and exhibition, Athens, Greece, 27 February–2 March 2006.

3. Grady, S.A.; Hussaini, M.Y.; Abdullah, M.M. Placement of wind turbines using genetic algorithms. *Renew. Energy* **2005**, *30*, 259–270. [[CrossRef](#)]
4. Göçmen, T.; van der Laan, P.; Réthoré, P.-E.; Diaz, A.P.; Larsen, G.C.; Ott, S. Wind turbine wake models developed at the Technical University of Denmark: A review. *Renew. Sustain. Energy Rev.* **2016**, *60*, 752–769. [[CrossRef](#)]
5. Renkema, D.J. Validation of Wind Turbine Wake Models Using Wind Farm Data and Wind Tunnel Measurements. Master's Thesis, Delft University of Technology, Delft, The Netherlands, 2007.
6. Bastankhah, M.; Porté-Agel, F. A new analytical model for wind-turbine wakes. *Renew. Energy* **2014**, *70*, 116–123. [[CrossRef](#)]
7. Mosetti, G.; Poloni, C.; Diviacco, B. Optimization of wind turbine positioning in large windfarms by means of a genetic algorithm. *J. Wind Eng. Ind. Aerodyn.* **1994**, *51*, 105–116. [[CrossRef](#)]
8. Marmidis, G.; Lazarou, S.; Pyrgioti, E. Optimal placement of wind turbines in a wind park using Monte Carlo simulation. *Renew. Energy* **2008**, *33*, 1455–1460. [[CrossRef](#)]
9. Bansal, J.C.; Farswan, P.; Nagar, A.K. Design of wind farm layout with non-uniform turbines using fitness difference based BBO. *Eng. Appl. Artif. Intell.* **2018**, *71*, 45–59. [[CrossRef](#)]
10. Tong, W.; Chowdhury, S.; Messac, A. A multi-objective mixed-discrete particle swarm optimization with multi-domain diversity preservation. *Struct. Multidiscip. Optim.* **2016**, *53*, 471–488. [[CrossRef](#)]
11. Song, D.R.; Fan, X.; Yang, J.; Liu, A.; Chen, S.; Joo, Y. Power extraction efficiency optimization of horizontal-axis wind turbines through optimizing control parameters of yaw control systems using an intelligent method. *Appl. Energy* **2018**, *224*, 267–279. [[CrossRef](#)]
12. Han, F.; Zhao, M.R.; Zhang, J.M.; Ling, Q.H. An improved incremental constructive single-hidden-layer feedforward networks for extreme learning machine based on particle swarm optimization. *Neurocomputing* **2017**, *228*, 133–142. [[CrossRef](#)]
13. Hou, P.; Hu, W.; Chen, C.; Soltani, M.; Chen, Z. Optimization of offshore wind farm layout in restricted zones. *Energy* **2016**, *113*, 487–496. [[CrossRef](#)]
14. Parada, L.; Herrera, C.; Flores, P.; Parada, V. Wind farm layout optimization using a Gaussian-based wake model. *Renew. Energy* **2017**, *107*, 531–541. [[CrossRef](#)]
15. Song, D.R.; Yang, J.; Cai, Z.L.; Dong, M.; Joo, Y.H. Model predictive control with finite control set for variable-speed wind turbines. *Energy* **2017**, *126*, 564–572. [[CrossRef](#)]
16. Scholbrock, A.; Fleming, P.; Schlipf, D. Lidar-enhanced wind turbine control: Past, present, and future. In Proceedings of the American Control Conference, Boston, MA, USA, 6–8 July 2016; pp. 1399–1406.
17. Song, D.R.; Yang, J.; Fan, X.; Liu, Y.; Liu, A.; Chen, G.; Joo, Y.H. Maximum power extraction for wind turbines through a novel yaw control solution using predicted wind directions. *Energy Convers. Manag.* **2018**, *157*, 589–599. [[CrossRef](#)]
18. Song, D.R.; Li, Q.; Cai, Z.; Li, L.; Jian, Y.; Mei, S.; Joo, H.Y. Model predictive control using multi-step prediction model for electrical yaw system of horizontal-axis wind turbines. *IEEE Trans. Sustain. Energy* **2018**. [[CrossRef](#)]
19. Capuzzi, M.; Pirrera, A.; Weaver, P.M. A novel adaptive blade concept for large-scale wind turbines. Part II: Structural design and power performance. *Energy* **2014**, *73*, 25–32. [[CrossRef](#)]
20. Shen, X.; Chen, J.G.; Zhu, X.C.; Liu, P.Y.; Du, Z.H. Multi-objective optimization of wind turbine blades using lifting surface method. *Energy* **2015**, *90*, 1111–1121. [[CrossRef](#)]
21. Chehour, A.; Younes, R.; Ilinca, A.; Perron, J. Review of performance optimization techniques applied to wind turbines. *Appl. Energy* **2015**, *142*, 361–388. [[CrossRef](#)]
22. Eminoğlu, U. Site-specific design optimization of horizontal-axis wind turbine systems using PSO algorithm. *Turk. J. Electr. Eng. Comput. Sci.* **2016**, *24*, 1044–1060. [[CrossRef](#)]
23. Mirghaed, M.R.; Roshandel, R. Site specific optimization of wind turbines energy cost: Iterative approach. *Energy Convers. Manag.* **2013**, *73*, 167–175. [[CrossRef](#)]
24. Luo, L.; Zhang, X.; Song, D.R.; Tang, W.Y.; Yang, J.; Li, L.; Tian, X.; Wen, W. Optimal design of rated wind speed and rotor radius to minimizing the cost of energy for offshore wind turbines. *Energies* **2018**, *11*, 2728. [[CrossRef](#)]
25. Fingersh, L.; Hand, M.; Laxson, A. *Wind Turbine Design Cost and Scaling Model*; Technical Report NREL/TP-500-40566; National Renewable Energy Laboratory (NREL): Golden, CO, USA, 2006.

26. Moné, C.; Hand, M.; Bolinger, M.; Rand, J.; Heimiller, D.; Ho, J. *2015 Cost of Wind Energy Review*; Technical Report NREL/TP-6A20-66861; National Renewable Energy Laboratory (NREL): Golden, CO, USA, 2017.
27. Liu, Y.; Chen, D.; Yi, Q. Wind Profiles and Wave Spectra for Potential Wind Farms in South China Sea. Part I: Wind Speed Profile Model. *Energies* **2017**, *10*, 125. [[CrossRef](#)]
28. Archer, C.L.; Vassel-Be-Hagh, A.; Yan, C.; Wu, S.; Pan, Y.; Brodie, J.F.; Maguire, A.E. Review and evaluation of wake loss models for wind energy applications. *Appl. Energy* **2018**, *226*, 1187–1207. [[CrossRef](#)]
29. European Wind Energy Association. *Wind Energy—the Facts: A Guide to the Technology, Economics and Future of Wind Power*; Routledge: Abingdon, UK, 2009.
30. Breton, S.P.; Geir, M. Status, plans and technologies for offshore wind turbines in Europe and North America. *Renew. Energy* **2009**, *34*, 646–654. [[CrossRef](#)]
31. 4cooffshore. Available online: <https://www.4coffshore.com/windfarms/xiangshui-demonstration-china-cn51.html> (accessed on 25 February 2019).
32. 4cooffshore. Available online: <https://www.4coffshore.com/windfarms/r%C3%B8nland-denmark-dk04.html> (accessed on 12 February 2019).
33. Dai, J.C.; Yang, X.; Wen, L. Development of wind power industry in China: A comprehensive assessment. *Renew. Sustain. Energy Rev.* **2018**, *97*, 156–164. [[CrossRef](#)]
34. Li, X.L.; Xie, C.J.; Quan, S.H.; Liang, H.; Wei, F. Energy management strategy of thermoelectric generation for localized air conditioners in commercial vehicles based on 48 V electrical system. *Appl. Energy* **2018**, *231*, 887–900. [[CrossRef](#)]



© 2019 by the authors. Licensee MDPI, Basel, Switzerland. This article is an open access article distributed under the terms and conditions of the Creative Commons Attribution (CC BY) license (<http://creativecommons.org/licenses/by/4.0/>).